Published February 17, 2014



# Transgenic kallikrein 5 mice reproduce major cutaneous and systemic hallmarks of Netherton syndrome

Laetitia Furio,[1,2] Simon de Veer,[1,2] Madeleine Jaillet,[1,2] Anais Briot,[2] Aurelie Robin,[2] Celine Deraison,[2] and Alain Hovnanian[1,2,3]

[1]Université Paris Descartes-Sorbonne Paris Cité, 75006 Paris, France
[2]INSERM UMR 1163, Laboratory of Genetic Skin Diseases, Imagine Institute, 75015 Paris, France
[3]Department of Genetics, Necker Hospital, 75015 Paris, France

**Netherton syndrome (NS) is a severe genetic skin disease in which absence of a key protease inhibitor causes congenital exfoliative erythroderma, eczematous-like lesions, and atopic manifestations. Several proteases are overactive in NS, including kallikrein-related peptidase (KLK) 5, KLK7, and elastase-2 (ELA2), which are suggested to be part of a proteolytic cascade initiated by KLK5. To address the role of KLK5 in NS, we have generated a new transgenic murine model expressing human KLK5 in the granular layer of the epidermis (Tg-*KLK5*). Transgene expression resulted in increased proteolytic activity attributable to KLK5 and its downstream targets KLK7, KLK14, and ELA2. Tg-*KLK5* mice developed an exfoliative erythroderma with scaling, growth delay, and hair abnormalities. The skin barrier was defective and the stratum corneum was detached through desmosomal cleavage. Importantly, Tg-*KLK5* mice displayed cutaneous and systemic hallmarks of severe inflammation and allergy with pruritus. The skin showed enhanced expression of inflammatory cytokines and chemokines, infiltration of immune cells, and markers of Th2/Th17/Th22 T cell responses. Moreover, serum IgE and Tslp levels were elevated. Our study identifies KLK5 as an important contributor to the NS proteolytic cascade and provides a new and viable model for the evaluation of future targeted therapies for NS or related diseases such as atopic dermatitis.**

CORRESPONDENCE
Alain Hovnanian:
alain.hovnanian@inserm.fr

Abbreviations used: AD, atopic dermatitis; ELA, elastase; GR, granular layer; ICAM1, intracellular adhesion molecule 1; KLK, kallikrein-related peptidase; LEKTI, lymphoepithelial Kazal-type inhibitor; MDC/Mdc, macrophage-derived chemokine; MMP, matrix metalloprotease; NS, Netherton syndrome; PAR2, protease-activated receptor 2; SC, stratum corneum; TARC/Tarc, thymus and activation regulated chemokine; TSLP/Tslp, thymic stromal lymphopoietin.

Netherton syndrome (NS; OMIM 256500) is an autosomal recessive disease regarded as one of the most severe heritable skin disorders affecting newborns. NS involves both cutaneous and immunological abnormalities, including congenital ichthyosiform erythroderma, pronounced peeling of the skin with detachment of the stratum corneum (SC) from the underlying epidermis, severe atopy with elevated serum IgE, and a characteristic hair shaft defect (Comel, 1949; Netherton, 1958; Judge et al., 1994; Hausser and Anton-Lamprecht, 1996). Collectively, these detriments represent a serious challenge to neonate health and promote frequent complications, including hypernatremic dehydration, failure to thrive and recurrent bacterial infections that can be life threatening. Previously, we established that the defective gene in NS is *SPINK5* (Chavanas et al., 2000), which encodes the multidomain protease inhibitor, lymphoepithelial Kazal-type inhibitor (LEKTI). To date, the majority of *SPINK5* mutations known to cause NS introduce a premature stop codon and result in a lack of detectable LEKTI expression (Hovnanian, 2013).

NS has brought into sharp focus the need to preserve the balance between proteolysis and inhibition in the epidermis. Similarly, LEKTI has emerged as a key regulator of epidermal proteolysis. Synthesized as a large (145-kD) polyprotein containing 15 Kazal domains, LEKTI is cleaved by furin to liberate a series of smaller fragments comprising one or more inhibitory units that target distinct protease subsets (Bitoun et al., 2003; Fortugno et al., 2011). LEKTI

C. Deraison's present address is Institut National de la Santé et de la Recherche Médicale, U1043 Toulouse, France.



The Rockefeller University Press $30.00
J. Exp. Med. 2014 Vol. 211 No. 3 499-513
www.jem.org/cgi/doi/10.1084/jem.20131797

Published February 17, 2014



inhibits several members of the kallikrein-related peptidase (KLK) serine protease family (KLK5, KLK7, and KLK14; Deraison et al., 2007; Fortugno et al., 2011). Additionally, LEKTI has been recently suggested to inhibit caspase-14 (Bennett et al., 2010). Collectively, these proteases are known to hold prominent roles in the SC. KLK5, KLK7, and KLK14 contribute to desquamation by degrading desmosomal cadherins such as desmoglein-1 and desmocollin-1 (Caubet et al., 2004; Fortugno et al., 2011) whereas caspase-14 is needed to complete the processing of filaggrin (Flg; Denecker et al., 2007; Hoste et al., 2011). KLK5 and KLK14 are also able to stimulate proinflammatory and proallergic signals via protease-activated receptor 2 (PAR2; Stefansson et al., 2008; Briot et al., 2009) and KLK5 and KLK7 are linked to the maturation of cathelicidin antimicrobial peptides (Yamasaki et al., 2006). Thus, LEKTI coordinates the timing of several important proteolytic events in epidermal physiology and its absence in NS causes dysregulation of multiple pathways.

The development of *Spink5*-deficient mice provided the first opportunity to unravel the complex pathophysiology of NS in an in vivo experimental model (Yang et al., 2004; Descargues et al., 2005; Hewett et al., 2005; Briot et al., 2009). *Spink5*$^{-/-}$ animals display a phenotype highly reminiscent of NS, replicating cutaneous and inflammatory aspects of the disease. Loss of LEKTI causes detachment of the SC from the underlying granular layer (GR) because of unopposed proteolytic activity and premature degradation of desmosomes (Yang et al., 2004; Descargues et al., 2005). Keratinocyte hyperproliferation, abnormal distribution of differentiation markers, accelerated Flg degradation, and lipid defects are also evident (Descargues et al., 2005; Bonnart et al., 2010). Concurrently, uncontrolled proteolytic activity propagates activation of epidermal proinflammatory and proallergic signaling pathways. In particular, proteolytic activation of PAR2 results in elevated expression of the pro-Th2 cytokine, thymic stromal lymphopoietin (TSLP), as well as several other proinflammatory and proallergic mediators (Briot et al., 2009).

Despite the neonatal lethality of Spink5-*deficient* mice (Yang et al., 2004; Descargues et al., 2005; Hewett et al., 2005), considerable progress has been made on detailing the biological pathways involved in NS pathophysiology. However, the significance of each protease implicated in the disease remains unclear. Loss of LEKTI leaves the activity of several proteases unopposed (Descargues et al., 2005; Deraison et al., 2007), many of which are capable of degrading desmosomes or filaggrin, and stimulating inflammation. Protease activation cascades present an additional layer of complexity by providing an avenue for proteases not targeted by LEKTI to be involved in NS, such as matriptase (Sales et al., 2010) and elastase-2 (ELA2; Bonnart et al., 2010). These unknowns conceal the identity of the most promising pharmaceutical targets in NS and represent a major obstacle in developing targeted therapies for NS and related skin disorders. Additionally, there is a current need to develop new animal models to study further aspects of NS pathophysiology, as *Spink5*$^{-/-}$ mice uniformly do not survive for more than a few hours after birth because of rapid dehydration (Yang et al., 2004; Descargues et al., 2005; Hewett et al., 2005).

In this study, we developed a new transgenic murine model expressing human KLK5 in the GR of the epidermis to assess the role of this protease in NS. KLK5 has been reported to cleave several desmosomal cadherins in vitro (Caubet et al., 2004; Descargues et al., 2006), to activate PAR2 in cultured keratinocytes (Stefansson et al., 2008) and has a prominent role in the proposed KLK proteolytic activation cascade (Brattsand et al., 2005). This study reveals that elevated KLK5 expression, even in the presence of functional Lekti, is sufficient to trigger the majority of the clinical hallmarks of NS. These findings establish the important role of KLK5 in NS pathophysiology and demonstrate its considerable potential as a therapeutic target in this severe genetic skin disorder.

## RESULTS

### KLK5 is overexpressed in the GR of Tg-*KLK5* mice

KLK5 is one of several proteases known to be overactive in NS, but its precise role in the disease remains to be defined (Descargues et al., 2005, 2006). To investigate the consequences of elevated KLK5 activity in vivo, we developed a transgenic murine model overexpressing human KLK5 under the control of the human involucrin promoter to target transgene expression in the GR of murine epidermis. The cDNA encoding human KLK5 full length sequence was fused to the FLAG tag and cloned downstream of the human involucrin promoter (Fig. 1 A). Animals carrying the transgene were identified using a PCR-based genotyping strategy as shown in Fig. 1 B. Western blot analysis using an anti-human KLK5 antibody confirmed expression of the exogenous protein in epidermal extracts of Tg-*KLK5* animals (Fig. 1 C). We identified this protein as being KLK5-Flag by Western blot analysis with an anti-Flag antibody (Fig. 1 E). To confirm correct targeting of KLK5 to the GR, immunostaining of skin sections using the anti–human KLK5 antibody was performed. Murine Klk5 was detected at the GR–SC interface in WT epidermis, indicating cross reactivity of the human antibody with murine Klk5. In Tg-*KLK5* epidermis, KLK5 staining was increased in the GR and SC, and faint in suprabasal cells (Fig. 1 D). Detection of the FLAG epitope in Tg-*KLK5* epidermis showed predominant expression of exogenous KLK5 in the GR and SC, and confirmed restricted expression of the transgene to the upper epidermis (Fig. 1 F).

### Tg-*KLK5* mice develop a skin barrier defect associated with growth delay, hair abnormalities, and constant scratching

NS patients classically present at birth with scaling and generalized erythroderma (Hausser and Anton-Lamprecht, 1996). At birth, Tg-*KLK5* animals were slightly smaller than WT littermates and showed mild erythroderma (Fig. 2 A). Tg-*KLK5* mice also showed significantly lower body mass than WT littermates (Fig. 2 A). To investigate epidermal barrier function in Tg-*KLK5* mice, we first examined the ability of the skin to prevent penetration of an external dye solution in a whole-mount assay. Tg-*KLK5* neonates exhibited more patches of

Published February 17, 2014



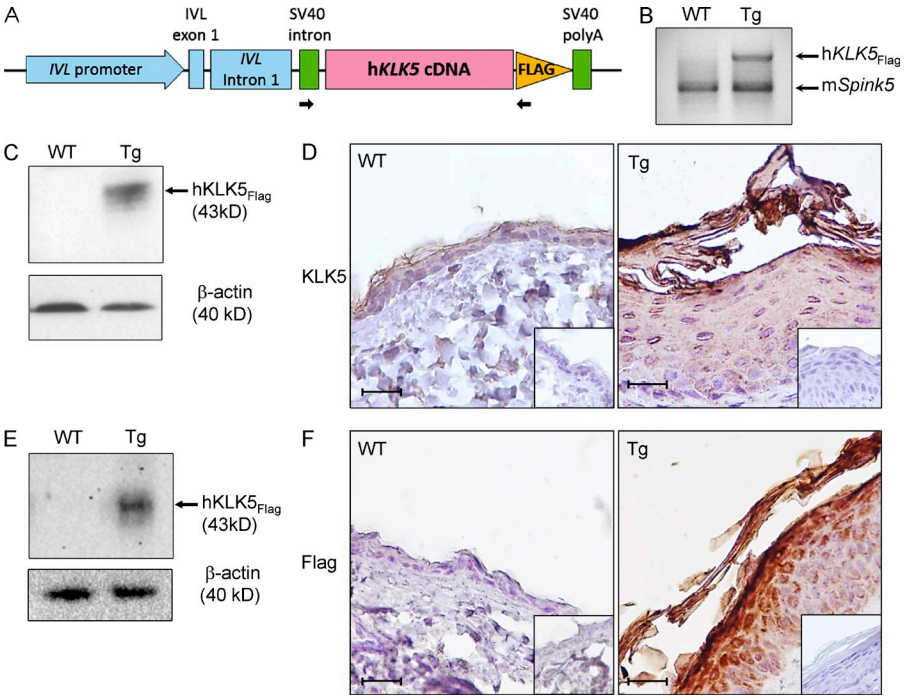


**Figure 1. Generation of transgenic-*KLK5* mice.** (A) Schematic structure of the transgene. The human full-length *KLK5* cDNA was fused at its 3′ end with the FLAG epitope and cloned downstream of the regulatory sequences of the human *IVL* promoter. (B) Transgenic mice were discriminated from WT animals by genomic PCR using primers specific for the SV40 intron and the FLAG epitope (arrows in A). The *Spink5* amplification was used as internal control. Transgenic KLK5 expression was confirmed by Western blot analysis using (C) anti-KLK5 and (E) anti-Flag antibodies on adult skin protein extracts. Localization of (D) KLK5 and (F) Flag expression by immunohistochemistry on adult WT and Tg-*KLK5* skin sections. Inserts at the bottom right of panel (D) and (F) show immunostaining with isotype controls. Bar, 25 µm.

blue staining compared with WT, mainly located on the neck, abdomen, muzzle, and ears, suggesting that the skin barrier was defective (Fig. 2 B). To measure the extent of the skin barrier defect, we tested the ability of the skin to prevent fluid loss by measuring transepidermal water loss (TEWL). Tg-*KLK5* neonates showed significantly higher TEWL compared with wild-type (Fig. 2 B).

During the first week of life, Tg-*KLK5* mice remained smaller than WT littermates with reduced body weight (Fig. 2 C). They developed exfoliative erythroderma and scaling of their entire body as shown at day 8 after birth in Fig. 2 (C and D). Their hair growth was also delayed (Fig. 2, C and D). TEWL measurement revealed that the difference in barrier function between WT and Tg-*KLK5* littermates had increased (Fig. 2 D). Although the severity of the phenotype was variable among Tg-*KLK5* littermates, growth delay, erythroderma, scaling, and sparse fur were observed in all animals at 1 mo of age (Fig. 2 E). To examine this further, we analyzed disease severity using an adapted Netherton area severity assessment (NASA) scheme which is used in the clinic for NS patients (Oji et al., 2005). Among Tg-*KLK5* mice at 1 mo of age, extension of the lesions varied from localized on the head and trunk to more generalized lesions (head, trunk, back, and limbs). The severity of erythema varied between mild and severe, scaling between moderate and severe, and lichenification (of the ears) between moderate and severe. Adult Tg-*KLK5* mice showed normal size and body weight but developed intense and continuous scratching (varying from moderate to severe), resulting in chronic and extensive erosions and crusts (Fig. 2 F, left). Another feature of NS is hair defects (brittle and sparse hair), which we could examine in Tg-*KLK5* mice as they survive the neonatal period. Body hair appeared thinner, lusterless, and spiky with flakes of dry skin on the fur. Cutting hair on the back revealed scaling underneath the fur (Fig. 2 F, right). Additionally, vibrissae were reduced, disoriented, bent, and short at birth (Fig. 2 G). Contrary to body hair which showed a delay in growth but appeared almost normal in nonlesional adult skin, whiskers stayed short and sparse as shown at 1 yr of age (Fig. 2 G). Finally, sub-cutaneous lumps were noticed around the neck and on the legs of Tg-*KLK5* mice (arrow; Fig. 2 H). These corresponded to enlarged lymph nodes, which are examined in further detail below (see also Fig. 7).

### hKLK5 expression triggers activation of the NS proteolytic cascade

In NS patients and *Spink5*-deficient mice, LEKTI deficiency leads to unopposed activity of several proteases, including KLK5, KLK7, and ELA2 (Descargues et al., 2005, 2006; Bonnart et al., 2010). To study whether overexpression of KLK5 led to global changes in skin proteolytic activity, we next analyzed protein extracts of adult skin by casein gel zymography. Several bands of proteolytic activity were detected and found to be enhanced in Tg-*KLK5* extracts (31, 28, 23, and 20 kD; Fig. 3 A). These bands have previously been identified as KLK5 (31 kD; Descargues et al., 2005), ELA2 (28 kD; Bonnart et al., 2010), and KLK7 (23–20 kD; Descargues et al., 2005), whereas KLK14 has been shown to comigrate with KLK7 (Stefansson et al., 2006). These data confirmed that heterologous KLK5 was active in Tg-*KLK5* epidermis and led to the activation of several additional protease targets.

To further explore the in vivo proteolytic activation cascade propagated by KLK5, we used peptide substrates known to be cleaved by downstream KLK proteases (KLK7 and KLK14;

Published February 17, 2014



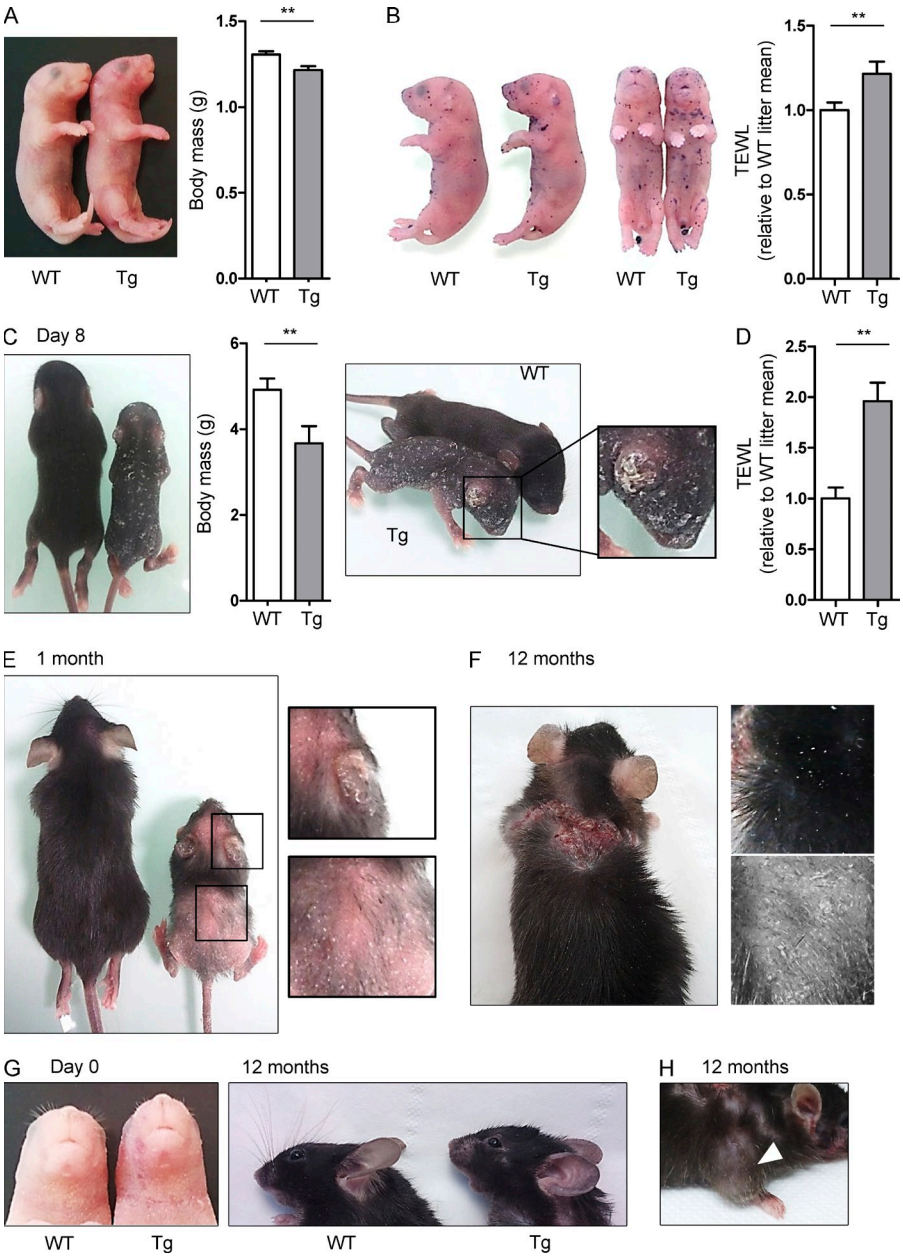


**Figure 2. Phenotype of Tg-*KLK5* mice combines a skin barrier defect, growth delay, hair abnormalities, and scratching lesions.** (A) Transgenic and WT littermate and body weight at birth. (B) Skin barrier–dependent dye exclusion assay using Toluidine blue in Tg-*KLK5* mice and WT littermate at birth and TEWL at birth. Mean TEWL value for WT was 9.3 g $m^{-2}$ $h^{-1}$ before normalization. Data from A–D are mean values ± SEM from at least 10 mice per genotype from 3 different litters. P-values were calculated using the Mann-Whitney *t* test. **, $P < 0.01$ comparing genotypes as indicated. (C) Phenotype and body weight of Tg-*KLK5* mice at day 8. (D) TEWL at day 8. Mean TEWL value for WT was 2.1 g $m^{-2}$ $h^{-1}$ before normalization. (E) Phenotype of Tg-*KLK5* mice at 1 mo of age. Tg-*KLK5* mice show a substantial but transient growth delay, erythroderma, scaling of the body and alopecia of the back, front, and head. (F) Phenotype at 1 yr of age. Persistent scratching leads to alopecic, erosive, and crusty injuries (F, left). Nonlesional skin shows scaling underneath the fur (right). (G) Whiskers aspects at birth (G, left) and in adults (G, right). (H) Swelling of regional lymph nodes (arrowhead) of Tg-*KLK5* mice at one year of age.

de Veer et al., 2012, 2013). Cleavage of these substrates was elevated by more than twofold in Tg-*KLK5* skin compared with WT (Fig. 3 B). Although we cannot entirely exclude substrate processing by other proteases, these results demonstrate that both trypsin- and chymotrypsin-like proteolytic activities are increased in Tg-*KLK5* skin.

Changes in MMP activity were also analyzed using gelatin gel zymography. Two groups of bands were detected, the lowest band for each being at 62 (MMP2) and 92 kD (MMP9). Therefore, it appeared that MMP2 activity was slightly lower and MMP9 activity was enhanced in Tg-*KLK5* samples (Fig. 3 C). The MW of these bands together with their sensitivity to EDTA identifies them as pro-, intermediate, and active forms of MMP2 and MMP9.

In situ zymography using BODIPY-FL-casein as a substrate showed that epidermal proteolytic activity was confined to the SC in WT skin, and that this activity was increased and extended to the GR in Tg-*KLK5* epidermis (Fig. 3 D). These results confirmed that heterologous KLK5 was active in the most differentiated layers of Tg-*KLK5* epidermis. Using BODIPY-FL-elastin as a substrate for in situ zymography, ELA activity was restricted to the GR and SC in WT epidermis, whereas it was slightly elevated and extended to suprabasal layers in Tg-*KLK5* (Fig. 3 E). FITC-gelatin in situ zymography showed low activity in WT epidermis, whereas activity was considerably increased in the GR and SC of Tg-*KLK5* (Fig. 3 F). In addition to increased proteolytic activity in the epidermis of Tg-*KLK5*, caseinolytic, elastinolytic,

Published February 17, 2014



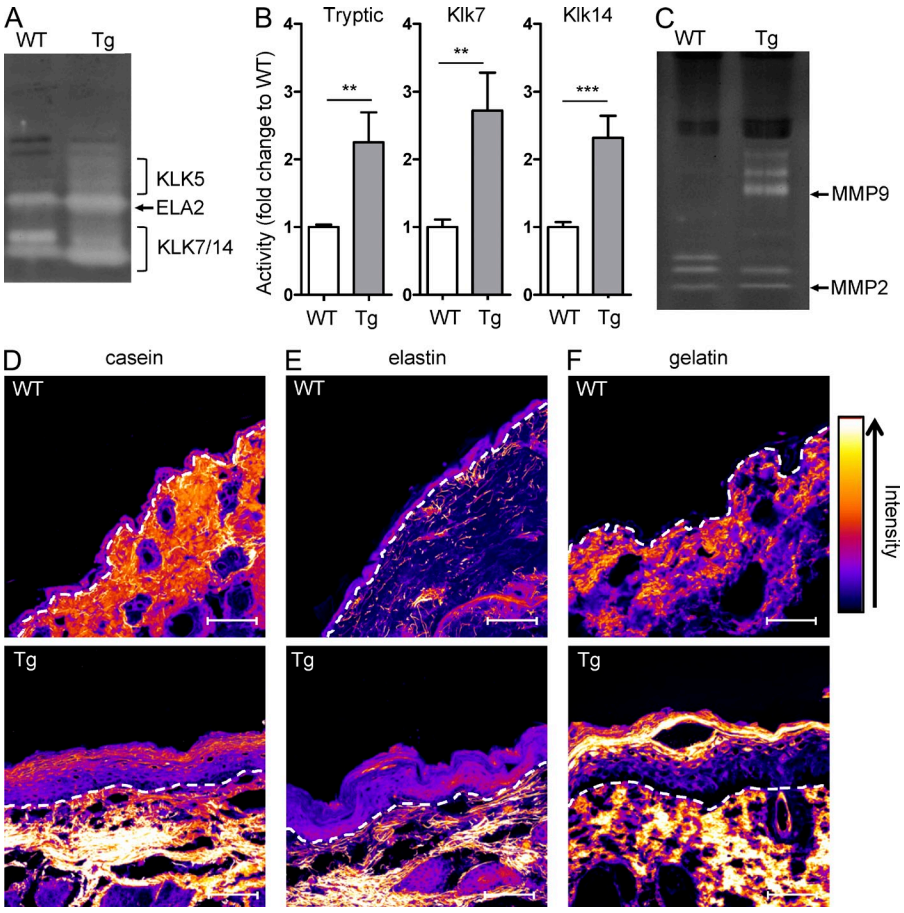


**Figure 3. KLK5 overexpression dysregulates an epidermal protease activation cascade.** (A) Proteolytic activity in skin extracts from WT and Tg-*KLK5* mice was examined by gel zymography using casein as an in-gel substrate. Areas of proteolytic activity are visible as clear bands against a dark background. The experiment shown is representative of five performed with three animals of each genotype. (B) Changes in proteolytic activity using a series of colorimetric substrates that target different proteases. Activity in WT and Tg-*KLK5* extracts was detected by measuring absorbance at 405 nm after overnight incubation with substrates for either tryptic proteases (KLK5, KLK14, and matriptase), KLK7 or KLK14. Data are shown as the mean ± SEM of duplicates for four mice per genotype. The experiment shown is representative of three. P-values were calculated using the Mann-Whitney *t* test. **, $P < 0.01$ and ***, $P < 0.001$ comparing genotypes as indicated. (C) Gel zymography using gelatin as an in-gel substrate. The experiment shown is representative of five performed with three animals of each genotype. (D–F) The localization of proteolytic activity was analyzed by in situ zymography on cryosections of WT and Tg-*KLK5* skin using internally quenched protein substrates. Cryosections were incubated with (D) BODIPY FL casein, (E) BODIPY FL elastin, or (F) FITC gelatin overnight and images were acquired using a Leica SP5 confocal laser scanning microscope. Fluorescence intensity data were transformed to a color gradient (as depicted) using ImageJ software. Dashed white lines represent the dermal–epidermal junction. The results shown are representative of experiments performed on at least five animals of each genotype. Bar, 25 µm.

and gelatinolytic activities were also increased in the dermis of these animals (Fig. 3, D–F). Overall, these data show that expression of hKLK5 in the GR of Tg-*KLK5* mice is sufficient to enhance KLK7, KLK14, and ELA2 activities in the epidermis, identifying KLK5 as an important contributor to the NS proteolytic cascade.

### KLK5 hyperactivity causes SC detachment through desmosome cleavage

NS patient skin shows characteristic acanthosis, hyperkeratosis, and SC detachment at the interface with the GR through desmosomal degradation. Histological analysis of Tg-*KLK5* epidermis revealed intercellular separation at the GR-SC boundary and detachment of the SC from the GR (Fig. 4 A, top). Compared with WT, Tg-*KLK5* epidermis constantly showed marked acanthosis, papillomatosis and hyperkeratosis before SC detachment. Interestingly, hair follicles were significantly reduced in number, hyperplastic and disorganized (Fig. 4 A, bottom). On electron microscopy sections, abnormal detachment of cells was evident in Tg-*KLK5* epidermis. Ultrastructural analysis showed that desmosomes were not cohesive at the interface between the GR and SC (Fig. 4 B). These structures were asymmetrically split with both dense plaques staying assembled. Contrary to *Spink5*$^{-/-}$ skin in which many remnant nuclei and keratohyalin granules were observed in corneocytes (Descargues et al., 2005), only mild parakeratosis, and no keratohyalin granules in the SC were observed after histological or electron microscopy analyses (Fig. 4 A).

Several studies have shown that KLK5 is able to degrade desmoglein-1 (Dsg-1) and desmocollin-1 (Dsc-1) in vitro, and therefore is regarded to contribute to the detachment of superficial corneocytes during desquamation (Suzuki et al., 1993; Brattsand and Egelrud, 1999; Caubet et al., 2004). We next analyzed the expression of the major desmosomal components including Dsg-1, Dsc-1, and desmoplakin (Dsp). Immunostainings against Dsg-1 and Dsc-1 on WT epidermal

Published February 17, 2014



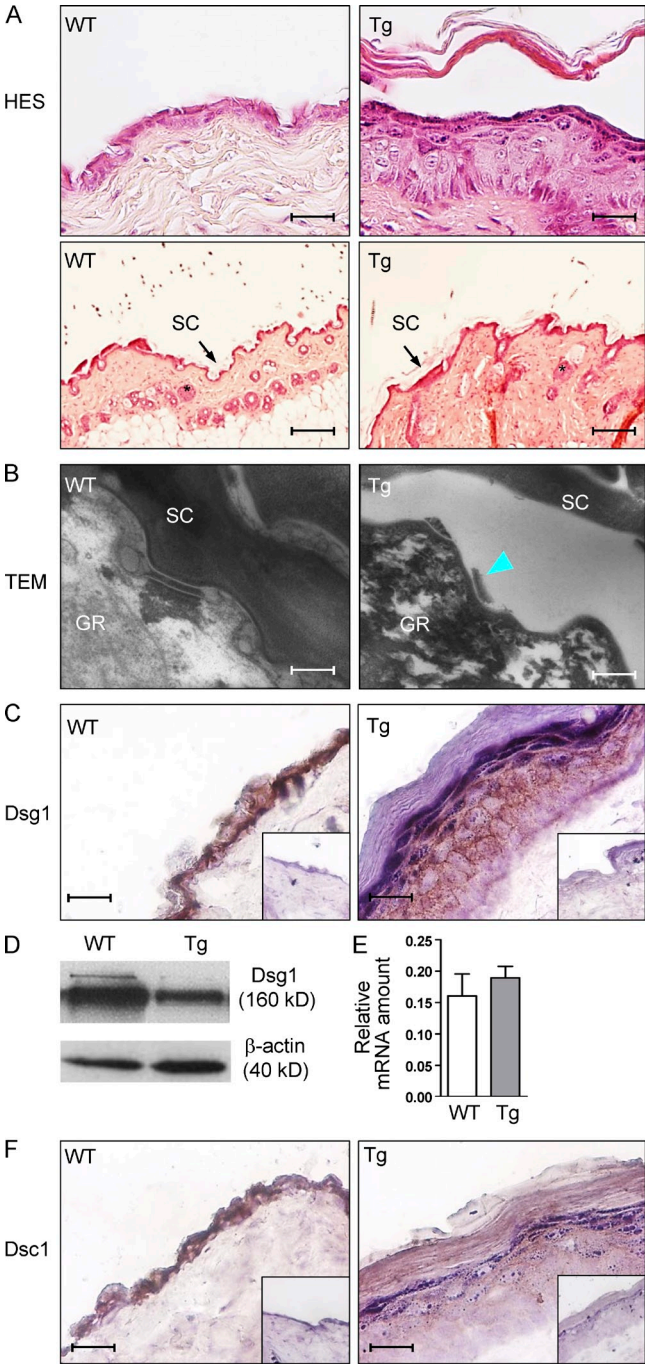


**Figure 4. SC detachment is a result of hyperactive hKLK5 and degradation of desmosomal components.** (A) Hematoxylin/eosin/safranin (HES) staining of adult WT and Tg-*KLK5* skin sections. Bar, 25 µm (top); 250 µm (bottom). (B) Ultrastructural analysis showing asymmetrical desmosome splits at the GR-cornified interface in Tg-*KLK5* epidermis (arrowhead). Bar, 200 nm. (C) Immunohistochemical analysis of desmoglein-1 (Dsg-1) expression in WT and Tg-*KLK5* skin sections. Bar, 25 µm. (D) Western blot analysis of Dsg-1 in Tg-*KLK5* epidermis compared with WT epidermis. Inserts at the bottom right show immunostaining with isotype control. (E) Quantitative RT-PCR of Dsg-1 relative to Hprt on mRNA extracted from Tg-*KLK5* and WT skin. Data are shown as the mean ± SEM of triplicate amplification for four mice per genotype. The experiment was performed three times. (F) Immunohistochemical analysis of desmocollin-1 (Dsc-1) expression in WT and Tg-*KLK5* skin sections. Bar, 25 µm. The immunohistochemistry and histology results shown are representative of experiments performed on at least five animals of each genotype.

sections revealed labeling limited to the cell border in the upper epidermis. In Tg-*KLK5* epidermis, cell dissociation correlated with a marked reduction of Dsg-1 and Dsc-1 stainings in suprabasal epidermis compared with WT (Fig. 4, C and F). Western blot analysis confirmed a lower amount of Dsg-1 in epidermal extracts from Tg-*KLK5* mice (Fig. 4 D). Transcript levels of *Dsg-1* analyzed by quantitative RT-PCR were not reduced in Tg-*KLK5* compared with WT mice, supporting the notion that reduced Dsg-1 expression resulted from proteolytic degradation (Fig. 4 E). In *Spink5*$^{-/-}$ mice, as well as in NS patients, we have previously shown that increased proteolytic activity leads to SC detachment at the GR–SC interface through degradation of Dsg-1, Dsc-1, and Dsp (Descargues et al., 2005, 2006). However, in Tg-*KLK5* epidermis, Dsp was not affected by KLK5 hyperactivity (unpublished data). Altogether, these data provide in vivo evidence that KLK5 hyperactivity initiates desmosomal component degradation and detachment of the SC from the GR.

### Tg-*KLK5* mice show no evidence for abnormal epidermal terminal differentiation

In addition to premature desquamation, NS skin shows impaired terminal differentiation with lipid abnormalities (Descargues et al., 2005, 2006; Bonnart et al., 2010). We next investigated epidermal terminal differentiation markers including involucrin, loricrin, and Flg in the epidermis of Tg-*KLK5* mice. Involucrin, which is an early marker of cornification, was expressed in the upper spinous layer and in the GR of WT epidermis (Fig. 5 A). In Tg-*KLK5* epidermis, involucrin showed the same pattern of expression but appeared to be extended due to acanthosis (Fig. 5 A). Immunostaining of loricrin, a later marker of cornification, was restricted to the upper GR and was not different between WT and Tg-*KLK5* (Fig. 5 B). Flg, which is mainly present in the GR and SC of WT epidermis, showed the same pattern of expression in Tg-*KLK5* epidermis (Fig. 5 C), unlike Flg over-degradation in *Spink5*$^{-/-}$ and Tg-*ELA2* epidermis (Descargues et al., 2005; Bonnart et al., 2010). By Western blot analysis, no difference could be detected in Flg processing between WT and Tg-*KLK5* (Fig. 5 D). We conclude that the skin barrier defect in Tg-*KLK5* mice is not associated with an abnormal differentiation pattern.

In adult WT and Tg-*KLK5* epidermis, nile red staining revealed uniform, linear lipophilic structures corresponding to corneocyte intercellular spaces. In WT, staining was thin and corresponded to the SC. In Tg-*KLK5*, multiple layers were seen, corresponding to hyperkeratosis (Fig. 5 E). Contrary to *Spink5*$^{-/-}$ and Tg-*ELA2* skin, no lipid droplets were observed in Tg-*KLK5*. Oil Red O, specific for free fatty acids, triglycerides, and esterified cholesterol showed staining only

Published February 17, 2014



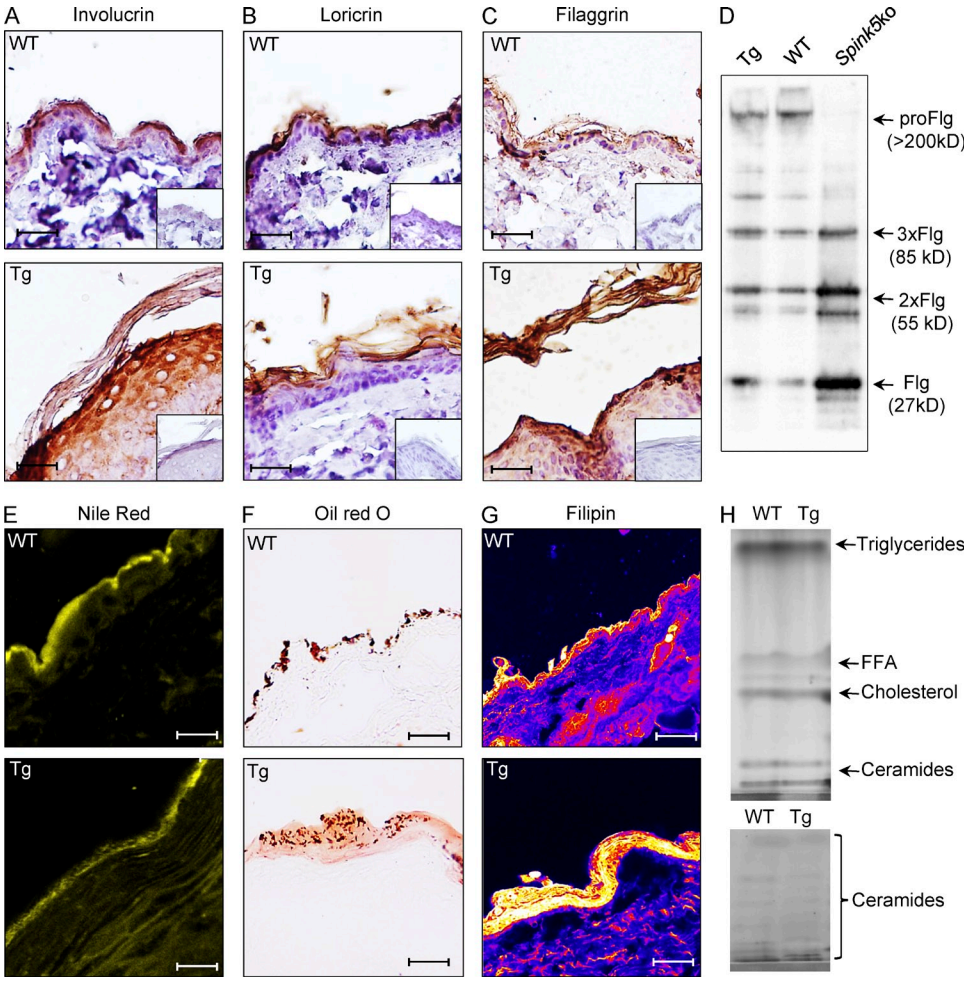


**Figure 5. Tg-*KLK5* skin does not show evidence of abnormal epidermal differentiation.** The expression of late-stage differentiation markers involucrin (A), loricrin (B), and Flg (C) was examined in paraffin-embedded skin sections from WT and Tg-*KLK5* (Tg) mice by immunohistochemistry. The inset on each panel shows the isotype control for each staining. Bar, 25 µm. The results shown are representative of experiments performed on at least five animals of each genotype. (D) Immunodetection of pro-Flg, Flg, and Flg-processing intermediate dimers (2xFlg) and trimers (3xFlg) in epidermal extract from an 8-d-old WT and Tg-*KLK5* animals and newborn Spink5$^{-/-}$. The experiment was performed three times with two animals of each genotype. The distribution of different lipid subsets was analyzed by staining with nile red (total lipids; E), Oil Red O (neutral lipids; F), and filipin (unesterified cholesterol; G). Fluorescence intensity data from filipin staining was transformed to a color gradient (as depicted) using ImageJ software. The results shown are representative of experiments performed on at least five animals of each genotype. Bar, 10 µm (E); 25 µm (F and G). (H) HP-TLC of lipids extracted from 8-d-old epidermis from WT and Tg-*KLK5* mice. The experiment was performed three times with one animal of each genotype.

in the SC for both WT and Tg-*KLK5* animals with no abnormal deposition in the skin (Fig. 5 F). Filipin, specific for unesterified cholesterol, intensely stained the SC in both WT and Tg-*KLK5* animals (Fig. 5 F). Increased intensity of staining in Tg-*KLK5* for Oil Red O and filipin could be attributable to marked hyperkeratosis (Fig. 5, F and G).

As epidermal lipid composition analysis requires isolation of the epidermis from the dermis, we used skin samples from 8-d-old mice, before hair emerges from the skin, for high performance-thin layer chromatography (HP-TLC). At this stage of analysis, hyperkeratosis is not as pronounced as in adult skin. No difference in lipid composition for triglycerides, free fatty acids, cholesterol, and ceramides was observed between WT and Tg-*KLK5* at day 8 (Fig. 5 H). Overall, these results demonstrate that KLK5 overexpression does not alter terminal differentiation reflected by differentiation marker expression or lipid abnormalities.

### KLK5 hyperactivity leads to cutaneous signs of allergy and inflammation

Uncontrolled proteolytic activity in NS leads to persistent activation of inflammatory signaling pathways in the epidermis. In NS epidermis, we previously uncovered a cell-autonomous process in which KLK5 directly activates PAR2 and induces NF-κB–mediated overexpression of thymic-stromal lymphopoietin (TSLP), intracellular adhesion molecule (ICAM-1), TNF, and IL-8 (Briot et al., 2009). Furthermore, *Spink5*$^{-/-}$-grafted skin is rich with proinflammatory and proallergic

Published February 17, 2014



molecules and is highly infiltrated by activated mast cells and eosinophils (Briot et al., 2009). Tg-*KLK5* nonlesional skin reproduced similar abnormalities, including infiltrates of T cells, mast cells and presence of eosinophil granulocytes in the dermis whereas none could be seen in WT (Fig. 6, A–C).

Disruption of the epidermal barrier stimulates elevated expression of an array of proinflammatory cytokines and activates signaling pathways that modulate keratinocyte differentiation and the immune response. To profile the proinflammatory environment induced by KLK5 hyperactivity, we performed a targeted transcript analysis using qRT-PCR. First, we examined the expression of prominent proinflammatory and proallergic cytokines in WT and Tg-*KLK5* nonlesional skin. Expression of the pro-Th2 cytokine Tslp, was significantly increased in Tg-*KLK5* skin, both at the mRNA and protein level (Fig. 6, D and E). Additionally, Tnf-α, Il-1β, and Icam-1 were all significantly increased at the mRNA level (Fig. 6 E). We next investigated the expression of molecules which are known to attract immune cells to the skin (Fig. 6 F). CCL17/TARC and CCL22/MDC are major pro-Th2 mediators that can recruit proallergic Th2 cells via the chemokine receptor CCR4 to the skin (Homey and Zlotnik, 1999). In Tg-*KLK5* skin, Ccl17 and Ccl22 mRNA levels showed a slight increase (Fig. 6 F). In contrast, Ccl8 (known to attract actors of allergy and inflammation) and Ccl20 (a chemoattractant for Th17 cells) showed significantly elevated expression in Tg-*KLK5* skin (Fig. 6 F). In addition, Tg-*KLK5* skin showed elevated expression of Il-6, Il-18, and Il-23 (Fig. 6 G).

Among the allergy/atopy-associated Th1/Th2 and Th17/Th22 cytokines, Il-4, Il-17, and Il-22 mRNA levels showed a significant increase in the skin of Tg-*KLK5* mice (Fig. 6 H). Additionally, genes known to be up-regulated by Th17 such as *Defb4* and *Cxcl1* (Nograles et al., 2008) showed elevated expression at the mRNA level in Tg-*KLK5* skin (Fig. 6 I). IL-17 and IL-22 are known to up-regulate the expression of S100A7, S100A8, and S100A9 in human keratinocytes (Boniface et al., 2005; Nograles et al., 2008). Increased levels

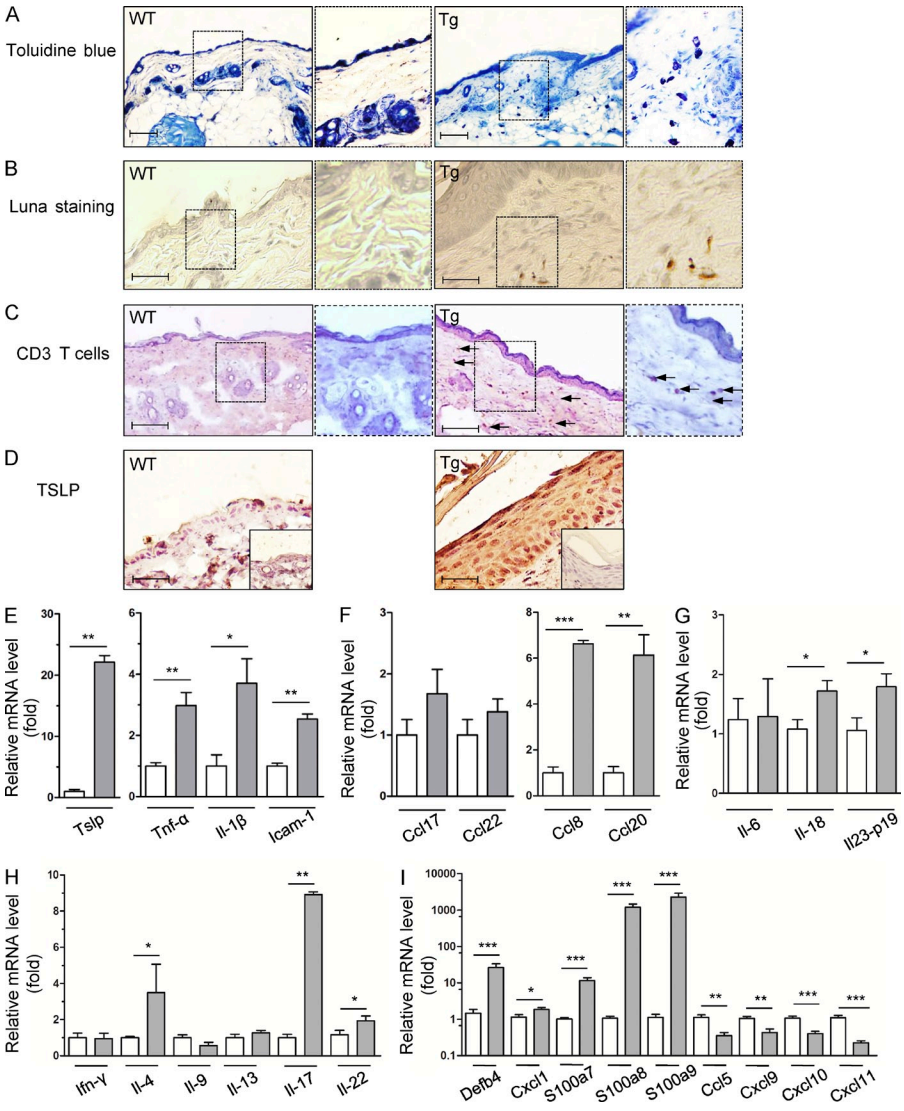


**Figure 6. Proallergic and inflammatory signals in Tg-*KLK5* nonlesional skin.** (A) Toluidine blue staining to detect infiltration of mast cells (stained purple). Bar, 100 µm. (B) Luna staining to detect polynuclear eosinophilic cells in adult nonlesional skin. Bar, 25 µm. (C) Immunohistochemical analysis of $CD3^+$ cells in adult nonlesional skin sections (arrows). Bar, 100 µm. (D) Immunohistochemical analysis of TSLP expression in adult WT and nonlesional Tg-*KLK5* skin. Bar, 25 µm. Insets at the bottom right show isotype controls. Stainings are representative of experiments performed three times with five animals of each genotype. (E–I) Relative mRNA expression of proinflammatory and proallergic cytokines and chemokines analyzed by quantitative RT-PCR on RNA extracted from adult nonlesional Tg-*KLK5* skin and WT skin. Data are shown as the mean ± SEM of triplicate amplification for at least six mice per genotype. Results are normalized to WT mean (set as 1.0). P-values were calculated using the Mann-Whitney *t* test. *, $P < 0.05$; **, $P < 0.01$; ***, $P < 0.001$. The experiment was performed three times.

Published February 17, 2014



of Il-17 and Il-22 transcripts in Tg-*KLK5* skin coincided with significant increases in S100a7, S100a8, and S100a9 mRNA expression (Fig. 6 I). Finally, the expression of genes up-regulated by Th1/IFN-γ such as *Ccl5*, *Cxcl9*, *Cxcl10*, and *Cxcl11* were all considerably reduced in Tg-*KLK5* skin (Fig. 6 I).

Collectively, these data demonstrate that dysregulated KLK5 activity in the skin is sufficient to induce cutaneous allergic inflammation. This involves up-regulation of Tslp, Icam-1, and Tnf-α and the production of chemokines known to attract mast cells, eosinophil granulocytes, and Th2/Th17/Th22 cells involved in allergy and inflammation.

### KLK5 hyperactivity triggers systemic allergy and inflammation

NS is a severe disease that is associated with a broad spectrum of severe atopic manifestations with high IgE levels. TSLP has been shown to be elevated in the serum of children with atopic dermatitis (Lee et al., 2010). Increased Tslp expression in Tg-*KLK5* skin led us to investigate the expression of this major pro-Th2 cytokine in the serum of adult Tg-*KLK5* mice. Tslp levels were significantly elevated in the serum of Tg-*KLK5* as compared with WT mice (Fig. 7 A). Additionally, we found significantly increased levels of total IgE in Tg-*KLK5* serum, and elevated total IgG, mainly due to increased IgG1 (Fig. 7 B). We next examined the morphology of lymphoid tissues including the spleen, thymus, and draining lymph nodes (cervical and inguinal). The spleen and lymph nodes were enlarged in Tg-*KLK5* mice, whereas the thymus appeared slightly smaller (Fig. 7 C). Lymph node enlargement resulted from hyperplasia as shown by the increase in the number of cells in inguinal nodes (Fig. 7 D).

The pro-Th2 cytokine TSLP, which is highly expressed in the skin and the serum of Tg-*KLK5* mice, is known to induce a proallergic microenvironment and to promote the differentiation of T helper (Th) 0 cells into proallergic Th2 cells (Soumelis et al., 2002). This led us to investigate whether T cells isolated from lymph nodes were Th1, Th2, and/or Th17 biased in Tg-*KLK5*. Phenotyping the cell populations from draining lymph nodes revealed an increased number of B cells, monocytes, dendritic cells, and T lymphocytes (unpublished data). Of the $CD4^+$ T cells isolated from lymph nodes, a higher proportion were IL-$4^+$, IL-$13^+$, TNF-$\alpha^+$, and IL-$17^+$–producing T cells as compared with WT (Fig. 7 E). Collectively, these data establish that the effects of KLK5 hyperactivity are not restricted to the skin. Indeed, overexpression of the protease specifically in the epidermis led to the production of allergy markers found in the serum and to the expansion of activated T cells in draining lymph nodes, as a consequence of skin inflammation and allergy.

## DISCUSSION

Netherton syndrome (NS) is a rare autosomal recessive skin disease with severe skin inflammation and scaling, a specific hair shaft defect and constant allergic manifestations. We and others previously described *Spink5*-deficient mice, which display key features of NS but die shortly after birth (Yang et al., 2004; Descargues et al., 2005; Hewett et al., 2005). Here, we developed a new model of NS by overexpressing KLK5 in the epidermis. These mice allowed us to both decipher the role of KLK5 hyperactivity in NS pathogenesis in vivo, and to provide a new and viable model to study further aspects of NS physiopathology, particularly those that become prominent after birth. We provide evidence here that overexpression of KLK5 in the epidermis leads to the development of the major NS hallmarks, confirming the role of KLK5 as a key contributor to the NS proteolytic cascade. In addition, we provide a new and viable mouse model recapitulating the hallmarks of NS.

In NS, the absence of LEKTI has been shown to result in unopposed activity of several proteases (Descargues et al., 2005, 2006; Bonnart et al., 2010). We show here that overexpression of human KLK5 in murine epidermis triggers major enhancement of the global proteolytic activity in the skin that overcomes the inhibitory capacities of Lekti. As our construct expresses KLK5 as a proprotease, this implies that it has been activated in vivo. It has recently been shown that matriptase can activate pro-KLK5 and pro-KLK7 in vitro (Sales et al., 2010). KLK5 has been shown to activate pro-KLK7, pro-KLK14, and pro-ELA2, as well as to amplify cascade initiation by activating pro-KLK5 in vitro (Brattsand et al., 2005; Bonnart et al., 2010). Using gel zymography and peptide substrates, we have shown that not only KLK5 activity but also KLK7, KLK14, and ELA2 activities were increased in Tg-*KLK5* skin. These results provide in vivo evidence that KLK5 can indeed activate KLK7, KLK14, and ELA2 as described by in vitro experiments (Brattsand et al., 2005; Bonnart et al., 2010). In addition, we observed an increase in MMP9 activity in Tg-*KLK5* skin. It is to our knowledge the first description of a functional link between MMP9 and KLK5, which is potentially mediated by PAR2 activation as demonstrated in transgenic *CAP1/Prss8 Par2*-deficient mice (Frateschi et al., 2011).

NS patients suffer from a profound skin barrier defect. Histopathologic examination of NS skin reveals a psoriasiform epidermis, associated with hyperkeratosis, hyperplasia of the subcorneal epithelium (acanthosis), and varying degrees of epidermal invaginations into the dermis (papillomatosis; Hausser and Anton-Lamprecht, 1996). These observations are consistent with the fact that skin barrier defects can induce compensatory hyperproliferative mechanisms resulting in hyperkeratosis and acanthosis. Another feature of NS epidermis is premature detachment of the SC from the GR as a result of desmosome cleavage (Descargues et al., 2005, 2006). These features are all seen in Tg-*KLK5* skin, including marked acanthosis, papillomatosis, and hyperkeratosis before SC detachment. Interestingly, IL-22, which is increased in chronic stages of atopic dermatitis induces epidermal hyperplasia (Nograles et al., 2008). The increased Il-22 expression observed in Tg-*KLK5* skin could thus contribute to acanthosis. In Tg-*KLK5* skin, the SC detachment occurs at the SC–GR interface as a result of desmosome cleavage through Dsg-1 and Dsc-1

Published February 17, 2014



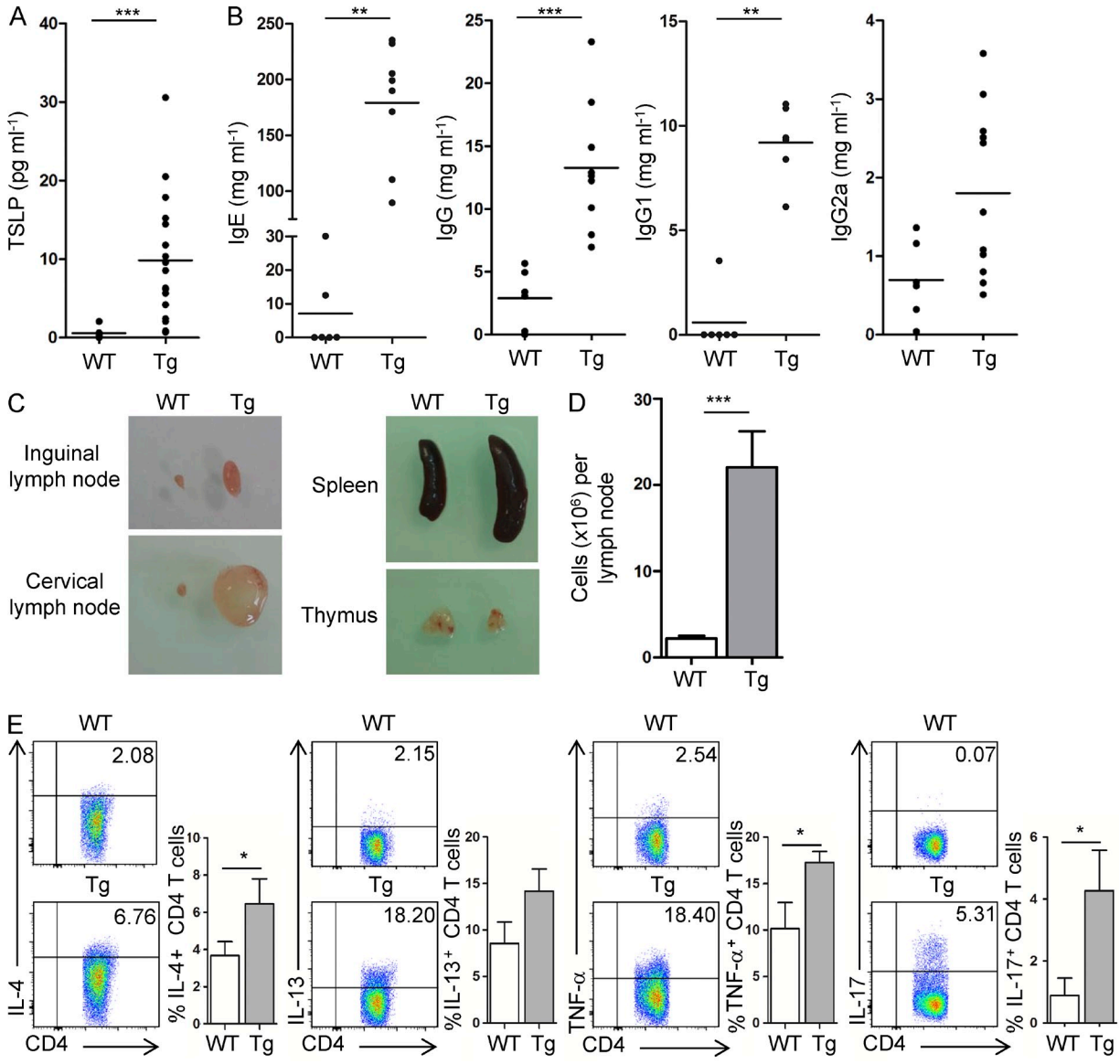


**Figure 7. Proallergic systemic inflammation in Tg-*KLK5* mice.** (A) Serum TSLP levels in WT and Tg-*KLK5* mice. Results shown are from at least 6 mice of each genotype. P-values were calculated using the Mann-Whitney *t* test. ***, $P < 0.001$. (B) IgE, IgG, IgG1, and IgG2 levels in the serum of adult mice. Results shown are from at least six mice of each genotype. **, $P < 0.01$; ***, $P < 0.001$. (C) Macroscopic appearance of inguinal and cervical lymph nodes (left), spleen (right), and thymus (right) in WT and Tg-*KLK5* adult mice. (D) Number of cells per inguinal lymph node in adult mice. Values correspond to mean ± SEM from nine animals per genotype. ***, $P < 0.001$. (E) Analysis of cytokine secretion from CD4 T cells after stimulation with PMA and ionomycin. Proportion of cells producing IL-4, IL-13, TNF-α, and IL-17 among the CD4 T cell population. Representative dot plots are shown. Values in the graphs are mean ± SEM from nine mice per genotype from two experiments. *, $P < 0.05$.

degradation as previously demonstrated in NS skin (Descargues et al., 2005, 2006). NS skin also exhibits impaired epidermal differentiation, with increased involucrin and loricrin expression, fewer keratohyalin granules, decreased Flg immunostaining in the GR and abnormal lipid structure and composition (Descargues et al., 2005, 2006; Bonnart et al., 2010). We have previously shown that ELA2 is hyperactive in NS skin and that transgenic mice overexpressing ELA2 in the GR displayed abnormal (pro-) Flg processing and impaired lipid lamellae structure (Bonnart et al., 2010). Of note, we did not observe major alterations in either epidermal terminal differentiation or Flg processing in Tg-*KLK5* mice, even though ELA2 activity was increased. One possibility could be that ELA2 activity did not reach the level of activation observed in the Tg-*ELA2* murine model as suggested by comparative elastin in situ zymography between Tg-*ELA2* and Tg-*KLK5* (unpublished data). Consistent with this, keratohyalin granules in Tg-*KLK5* were still present, in contrast to Tg-*ELA2* where they were absent (Bonnart et al., 2010). Recently, KLK5 was shown to directly process pro-Flg in vitro

Published February 17, 2014



(Sakabe et al., 2013). The fact that no significant decrease in pro-Flg was observed in Tg-*KLK5* animals suggests that regulation of pro-Flg processing by KLK5 is more complex and involves additional factors in vivo. The presence of Lekti in Tg-*KLK5* mice could imply that KLK5 and other pro-Flg processing proteases, such as caspase 14, remained sufficiently regulated during terminal differentiation to prevent Flg overdegradation. The observation that Tg-*KLK5* mice reproduce major abnormalities of NS supports an important role for KLK5 in the disease. However, not all features are observed, suggesting that additional proteases could be involved in the complete phenotype.

NS patients show failure to thrive in infancy and short stature. In a similar way, Tg-*KLK5* mice displayed a lower weight at birth and a growth delay. However, this delay was only transient and mice had a nearly normal weight and size at 2 mo of age. Several KLKs, including KLK5, are known to cleave growth hormone (GH) and to be present in the pituitary gland (Komatsu et al., 2007). It has been suggested that in NS patients the absence of LEKTI leads to higher proteolytic processing of GH, which may become biologically inactive (Komatsu et al., 2007). As we do not expect transgene expression in the pituitary gland and Lekti is still present in Tg-*KLK5*, it is possible that other factors contribute to the growth delay in Tg-*KLK5* mice. Another characteristic feature of NS patients is a specific hair shaft defect (trichorrhexis invaginata) that leads to sparse, brittle, and spiky hair. In Tg-*KLK5* animals, we observed an apparent thinning of body hair, which had a lusterless and spiky appearance. As in newborn *Spink5*$^{-/-}$ mice (Descargues et al., 2005), Tg-*KLK5* whiskers were scarce, disoriented, bent, and short. Existing murine models such as *Cathepsin L*$^{-/-}$ or *Matriptase*$^{-/-}$ have shown that hair follicle morphogenesis is a protease-dependent process (Roth et al., 2000; List et al., 2002). This viable murine model will allow the mechanisms underlying hair follicle abnormalities in NS to be deciphered.

In NS patients, atopic features with elevated IgE are constant during infancy and adulthood. These include eczematous-like lesions, allergic asthma, allergic rhinitis, urticaria, and angiodema (Sun and Linden, 2006). Only a few immunological studies have been reported in NS patients to date (Judge et al., 1994; Stryk et al., 1999; Renner et al., 2009). In these studies, a constant finding is elevated specific IgE levels to common allergens, although a proallergic Th2 skew has not been consistently found. Studies on *Spink5*$^{-/-}$ skin have been limited to grafting experiments on WT mice and have shown enhanced expression of proinflammatory cytokines, such as Il-1β, Tnf-α, IL-8, and Icam-1 and proallergic mediators, such as Tslp, Ccl17 (Tarc), and Ccl22 (Mdc; Briot et al., 2009). We have previously shown that increased TNF, IL-8, ICAM-1, and TSLP expression is an intrinsic property of NS keratinocytes as a result of the KLK5–PAR2–NF-κB pathway (Briot et al., 2009). The proinflammatory and proallergic cytokines overexpressed in NS epidermis play an active role in recruiting inflammatory cells to the skin, including mast cells and eosinophils whose numbers are significantly increased in *Spink5*$^{-/-}$ skin grafts (Briot et al., 2009). These features of severe cutaneous inflammatory and atopic manifestations are prominent in Tg-*KLK5* mice. Our results establish that KLK5 overactivity in murine epidermis is sufficient to induce a proallergic and proinflammatory environment.

In skin of atopic dermatitis patients, TSLP expression is associated with the migration of Langerhans cells to the draining lymph nodes. TSLP-activated dendritic cells have been shown to induce naive T cells to differentiate into "allergic" Th2 cells producing IL-4, IL-5, IL-13, and TNF (Soumelis et al., 2002). We have previously shown that NS keratinocytes show high expression of TSLP (Briot et al., 2009). Consistent with this observation, we showed that TSLP expression was also strongly enhanced in Tg-*KLK5* skin. Normal human keratinocytes do not express detectable levels of TARC and MDC, contrary to NS and AD keratinocytes (Horikawa et al., 2002; Tsuda et al., 2003; Briot et al., 2009). These two chemokines can recruit Th2 cells via CCR4 to the skin, defining them as major pro-Th2 mediators (Homey and Zlotnik, 1999). In NS keratinocytes, we have previously shown that MDC and TARC are not induced by KLK5 and PAR2 activation (Briot et al., 2009). We have confirmed this observation in vivo because Tg-*KLK5* skin exhibits only a slight increase of these two chemokines. However, the presence of IL-4 in Tg-*KLK5* skin reflects the presence of Th2 cells. This suggests that slightly elevated Mdc and Tarc levels, when combined with the inflammatory environment are sufficient to recruit Th2 cells to the skin of Tg-*KLK5* mice.

We also uncovered the presence of Th17 and Th22 cells in Tg-*KLK5* skin. In inflammatory diseases, such as psoriasis, it has been shown that the presence of "inflammasome related" cytokines such as IL-1β and IL-18 could synergize with IL-23 to promote Th17 cell differentiation (Mills et al., 2013). In Tg-*KLK5* skin, we found elevated expression of Il-1β, Il-18, and Il-23, which could explain the presence of Th17 cells. The treatment of healthy keratinocytes with TNF induces the expression of CCL20, a molecule involved in Th17 recruitment (Kennedy-Crispin et al., 2012). It is thus possible that enhanced Tnf-α and Il-1β production in Tg-*KLK5* contributes to Ccl20 expression leading to Th17 recruitment. Of note, IL-17 has been shown to induce the secretion of proinflammatory cytokines (IL-1β and IL-6), antimicrobial peptides, and several chemokines including IL-8 and CCL20 in human keratinocytes. In addition, the induction of CCL20 by keratinocytes has been suggested as a mechanism that maintains Th17 cells in skin (Perera et al., 2012). We have also found increased expression of *Defb4*, *Cxcl1*, *S100a7*, *S100a8*, and *S100a9* in Tg-*KLK5* skin, which are genes known to be induced by Il-17 and Il-22. A similar inflammatory profile is found in atopic dermatitis in which, in addition to Th2, Th22 and Th17 play important roles in the pathogenesis of the disease (Guttman-Yassky et al., 2013; Suárez-Fariñas et al., 2013). These observations support the contribution of Th17 and Th22 cells to skin inflammation in the Tg-*KLK5* murine model.

Unlike *Spink5*$^{-/-}$ mice, Tg-*KLK5* mice are viable, which allowed us to investigate signs of allergy in the serum. We

Published February 17, 2014



found elevated Tslp and IgE concentrations that reflect the Th2 cytokine-mediated IgE class switch of B cells. Thus, our results show that the effects of dysregulated KLK5 activity are not restricted to Tg-*KLK5* skin. In Tg-*KLK5* mice, continuous scratching led to alopecic, erosive, and crusty skin lesions. These observations are highly relevant to NS patients who show constant, often severe and disabling pruritus. Persistent itch causes sleeplessness and scratching, which further aggravate skin lesions. A well-established mediator of itching is PAR2 activation (Steinhoff et al., 2003). Several serine proteases capable of activating PAR2 are present in Tg-*KLK5* skin, including KLK5, KLK14 in the epidermis, and tryptase from infiltrating mast cells. Tg-*CAP1/Prss8* mice display a similar itchy phenotype, which could be rescued by PAR2 knock-down (Frateschi et al., 2011). In Tg-*KLK7* mice, which develop chronic dermatitis, itching does not respond to antihistamine therapy and is also potentially attributable to PAR2 activation (Hansson et al., 2002).

In summary, we have generated a new and viable murine model that recapitulates the major cutaneous and systemic hallmarks of NS and validates KLK5 as a promising target for NS treatment. Accordingly, successful inhibition of KLK5 has the potential to reduce the skin barrier defect as well as features of inflammation and allergy. Furthermore, this model will allow the study of further aspects of NS pathophysiology that are currently not well understood, such as growth delay, immune system dysregulation, and hair defects. It will also be instrumental for preclinical testing of therapies for NS and related diseases that involve a skin barrier defect and severe atopic manifestations. Indeed, atopic dermatitis shows several similarities with NS, including increased skin barrier permeability and elevated TSLP, which lead to a Th2-biased response and high serum IgE. Collectively, our results show that the Tg-*KLK5* murine model shares important similarities with human atopic dermatitis. Therapies aiming at controlling these dysregulated pathways could be evaluated in vivo using the Tg-*KLK5* murine model.

## MATERIALS AND METHODS

**Generation of KLK5 transgenic mice.** This work was approved by the Commission de Génie Génétique (01–10-08, agreement number 4858) and all experiments were performed in accordance with the required guidelines and regulations. The full-length cDNA encoding human *KLK5* (I.M.A.G.E. clone 100020682) was amplified by RT-PCR. The FLAG octopeptide epitope was added to the 3′ end of the resulting product followed by NotI restriction sites to both ends. After digestion with NotI, this construct was inserted into the *IVL* promoter vector (pH3700-pL2; gift from J. Segre, National Human Genome Research Institute, Bethesda, Maryland; Carroll and Taichman, 1992; Carroll et al., 1993) and validated by sequencing. The transgene (comprising the *IVL* promoter and human $KLK5_{FLAG}$ construct) was excised from pH3700-pL2 by digestion with SalI, purified and injected into the pronuclei of fertilized oocytes from (C57BL/6 x CBA) F1 mice, and finally implanted into pseudopregnant females. First generation offspring were genotyped by isolating genomic DNA from mouse tail samples using the Nucleospin Tissue kit (Macherey-Nagel) and performing PCR using allele-specific primers designed to detect the transgene or an internal PCR control. The founder mouse was crossed and backcrossed with wild-type C57BL/6 animals to establish the transgenic line according to the International Committee on Standardized Genetic Nomenclature for Mice. Transgenic mice were named Tg-*KLK5* for the following study.

**TEWL measurement.** TEWL was measured using an EP1 evaporimeter (ServoMed) as previously described (Descargues et al., 2005).

**Barrier function assay.** Euthanized newborn mice were immediately subjected to graded methanol dehydration and subsequent rehydration as previously described (Ekholm et al., 2000). Pups were then washed in PBS for 1 min, stained in 0.1% toluidine blue (Sigma-Aldrich) for 1 h at room temperature, destained for 15 min in PBS, and analyzed.

**RNA isolation, RT, and quantitative real-time PCR.** Murine skin was crushed in RLT buffer (QIAGEN) using an Ultra-Turax, after which RNA was isolated using the RNeasy mini kit (QIAGEN). Complementary DNA was synthesized by reverse transcription from 1 µg total RNA using M-MLV Reverse transcription (Invitrogen). Quantitative real-time PCR was performed on an ABI prism 7500 Sequence Detection system (Applied Biosystems) using qPCR MesaGreen Mastermix (Eurogentec). The expression of target genes was normalized to murine hypoxanthine phosphoribosyl transferase (*Hprt*). Primer sequences can be obtained on request from the authors. Data were analyzed using 7500 software v2.0.6. (Applied Biosystems).

**Antibodies.** Antibodies used for Western blot analysis and immunohistochemistry were: Actin (A5441; Sigma-Aldrich), Flag (F7425; Sigma-Aldrich); Desmocollin-1 (sc18115; Santa Cruz Biotechnology, Inc.); Desmoglein-1 (sc20114; Santa Cruz Biotechnology, Inc.); Flg (PRB-417P; Covance); KLK5 (ab7283; Abcam); Involucrin (sc15230; Santa Cruz Biotechnology, Inc.); Loricrin (PRB-145P; Covance); TSLP (AF555; R&D Systems); and CD3 (ab5690; Abcam).

**Western blotting.** For Western blot analysis, skin was crushed in protein extraction buffer (50 mM Tris-HCl, pH 8.5, 5 mM EDTA, 150 mM NaCl, 0.1% Nonidet-P40, and Protease Inhibitor Cocktail Tablets [Complete, Roche]) using an Ultra-Turax. Lysates were clarified by centrifugation (13,000 *g*, 4°C for 30 min) to remove insoluble material. For Flg Western blot analysis, proteins were extracted using 50 mM Tris-HCl, pH 8.0, 8 M urea, 10 mM EDTA, and Protease Inhibitor Cocktail Tablets. Protein content in each sample was measured by Bradford assay (Bio-Rad Laboratories) according to the manufacturer's instructions. Protein fractions were mixed with Laemmli buffer, incubated for 5 min at 90°C, and then separated by SDS-PAGE. For KLK5, Flag, and Dsg-1 Western blots, 5 µg of proteins (for Flg, 1.5 µg of proteins) were loaded on a 4–12% precast gel (Invitrogen). After migration, proteins were transferred to Hybond-ECL membranes (GE Healthcare). After incubation with primary and secondary antibodies, enhanced chemiluminescence detection was performed as recommended by the manufacturer (Thermo Fischer Scientific).

**In situ zymography.** Skin cryosections (5-µm thickness) were mounted on glass slides, rinsed with 2% Tween 20 in PBS and incubated at 37°C overnight with 10 µg $ml^{-1}$ BODIPY FL casein (Life Technologies), 100 µg $ml^{-1}$ BODIPY FL elastin (Life Technologies) or 4 µg $ml^{-1}$ FITC-gelatin (Life Technologies) in 50 mM Tris-HCl, pH 8.0. Sections were rinsed with PBS and visualized using a Leica TCS SP5 AOBS confocal microscope. Data were analyzed using ImageJ (National Institutes of Health) software.

**Proteolytic activity assays.** For proteolytic activity assays, skin was crushed in 1 M acetic acid using an Ultra-Turax. After overnight extraction at 4°C, insoluble material was removed by centrifugation (13,000 *g*, 4°C for 30 min) and the supernatant was dried using a Speed-Vac. Proteins were resuspended in water overnight at 4°C and clarified by centrifugation (13,000 *g*, 4°C for 30 min). Protein content was determined by Bradford assay (Bio-Rad Laboratories).

For gel zymography, 10 µg of protein extracts were loaded onto casein/acrylamide copolymerized gels (15% acrylamide, 0.1% α-casein; Sigma-Aldrich)

Published February 17, 2014



or gelatin/acrylamide copolymerized gels (10% acrylamide and 0.1% gelatin; Sigma-Aldrich) for electrophoresis. After separation by SDS-PAGE, gels were washed with 2.5% Triton X-100 (two times for 30 min) and incubated for 24 h at 37°C in reaction buffer (50 mM Tris-HCl, pH 8.0). Buffer for gelatin zymography additionally contained 10 mM $CaCl_2$. Gels were stained with 1% Coomassie Brilliant blue G250.

Additionally, proteolytic activity was assessed using colorimetric peptide substrates that are preferentially cleaved by different proteases. Acetic acid skin extracts (25 µg) were added to assay buffer (0.1 M Tris-HCl pH 8.0, 0.005% Triton X-100, 0.05% sodium azide) in 96-well plates (final volume 200 µl). Substrates used were 150 µM Ac-YASR-pNA (cleaved by several trypsin-like serine proteases including KLK5, KLK14 and matriptase), 150 µM KHLY-pNA (cleaved by KLK7) and 150 µM Ac-WAVR-pNA (cleaved by KLK14; de Veer et al., 2012, 2013). Plates were incubated at 37°C overnight and activity was analyzed by measuring the increase in absorbance at 405 nm compared with substrate only controls.

**Histological, immunohistochemical, and immunofluorescence analysis.** Skin samples were snap frozen in liquid nitrogen in Tissue-Tek O.C.T. (Thermo Fischer Scientific) or fixed in 10% buffered formalin and embedded in paraffin. Hematoxylin/eosin/safranin, toluidine blue, and luna staining were performed on paraffin-embedded sections using standard histological techniques. For antigen retrieval, paraffin-embedded sections were boiled in 10 mM citrate buffer, pH 6.0, for 20 min ( Flg or TSLP immunostaining) or treated with S1700 solution (Dako) for 45 min (KLK5, Flag, Involucrin, or Loricrin immunostaining). Desmoglein-1, Desmocollin-1, and CD3 immunohistochemistry was performed on skin cryosections. Signal was detected using the appropriate horseradish peroxidase (HRP)–conjugated polymer (En Vision System; Dako).

**Transmission electron microscopy analysis.** Skin samples were fixed in 4% paraformaldehyde and 2% glutaraldehyde, rinsed in Sorensen buffer, post-fixed in 2% aqueous $OsO_4$, dehydrated in graded ethanol solution, and embedded in epon. Ultrathin sections were counterstained with uranyl acetate and lead citrate. Examination was performed with a 1011 transmission electron microscope (Jeol Inc., Japan). Acquisition and processing were performed with an Erlangshen CCD camera (Gatan Inc.) and Digital Micrograph software (Gatan Inc.).

**Lipid analyses.** For nile red staining, cryosections were incubated with 2.5 µg $ml^{-1}$ nile red in 75% glycerol for 5 min and mounted. Filipin staining was performed on cryosections using 50 µg $ml^{-1}$ filipin in 75% glycerol and 25% water (30 min incubation). Slides were rinsed twice with PBS and mounted with aqueous mounting medium. For Oil Red O staining, cryosections were incubated for 10 min in 60% isopropanol followed by staining with 0.3% (wt/vol) Oil Red O in 60% isopropanol (20 min). Sections were subsequently rinsed with water and mounted with aqueous mounting medium. Filipin and nile red stainings were visualized using a Leica TCS SP5 AOBS confocal microscope and data were analyzed using ImageJ. Oil Red O stainings were visualized using a white-light microscope. Lipid composition analysis was performed using HP-TLC as previously described (Bonnart et al., 2010).

**Measurement of serum TSLP and immunoglobulin levels.** Sera were analyzed by ELISA for TSLP, total IgG, IgG1, IgG2a, and IgE levels. Serum TSLP was measured using the murine TSLP Quantikine ELISA kit (R&D Systems) according to the manufacturer's instructions. For immunoglobulin analysis, ELISA plates were coated overnight with rat anti–mouse IgG (2.5 µg $ml^{-1}$, LO-MG-COC-2), IgG1 (1.25 µg $ml^{-1}$, LO-MG1-13) or IgG2a (5 µg $ml^{-1}$, LO-MG2a-7) antibodies (Southern Biotech). Plates were blocked with 1% BSA in PBS and incubated with serial dilutions of mouse sera, followed by anti-Ig PO HRP-conjugated secondary (1/2000, Southern Biotech). Signal was developed by incubation with 3,3′,5,5′–tetramethylbenzidine substrate (Fluka). For IgE, plates were coated overnight with 3 µg $ml^{-1}$ rat anti–mouse IgE (LO-ME-3), blocked with 1% BSA in PBS, and incubated with serial dilutions of mouse sera, followed by biotinylated rat anti–mouse IgE antibody (1/2000; Southern Biotech). Signal was developed by addition of streptavidin-HRP conjugate (1/2000; Interchim). All samples were analyzed in duplicate or triplicate by measuring the absorbance at 450 nm using a microplate reader (Versamax; Molecular Devices). Concentrations were calculated using standard curves generated with known dilutions of mouse IgG, IgG2a, IgG1 (Southern Biotech), and IgE (BD).

**Flow cytometry.** Single-cell suspensions were prepared from inguinal lymph node extracts. Surface antigen staining was performed using the following antibodies (eBioscience): anti-CD45 (clone 30-F11), anti-CD4 (clone RM4-5), anti-CD8 (clone 53–6.7), and anti-TCRγ (clone H57-597). For intracellular cytokine staining, isolated cells were activated in complete RPMI containing 0.5 µg $ml^{-1}$ phorbol 12 myristate 13-acetate (PMA), 0.5 µg $ml^{-1}$ ionomycin and 10 µg $ml^{-1}$ brefeldin A (all from Sigma-Aldrich) for 4 h. After surface staining, cells were fixed and permeabilized using Cytofix/Cytoperm solution (BD). Cells were washed in perm/wash buffer and incubated for 30 min at 4°C with different antibody combinations specific for murine cytokines (all from eBioscience) diluted in perm/wash buffer: anti-Il4 (clone 11B11), anti–IL-13 (clone eBio13A), anti-Il17 (clone eBio17B7), and TNF (clone MP6-XT22). Immunostained cells were analyzed by flow cytometry using a FACS Aria flow cytometer (BD).

**Statistical analysis.** Experiments were repeated at least three times and p-values were calculated using the Mann–Whitney *t* test. $P < 0.05$ was considered significant.

We are grateful to Julia Segre for providing the pH3700-pL2 vector. We thank Anne Huchenq-Champagne and Sylvie Appolinaire-Pilipenko for the transgenesis and cryoconservation platform (IFR150, Toulouse, France).

This work was supported by the French Ministry of Health, the Agence Nationale de la Recherche (ANR-08-GENO-033), and the Fondation pour la Recherche Médicale (FRM-DAL20051205066). S. de Veer received an international travel grant from the Fondation René Touraine.

The authors have no financial conflict of interest to declare.

**Submitted: 27 August 2013**
**Accepted: 15 January 2014**

## REFERENCES

Bennett, K., R. Callard, W. Heywood, J. Harper, A. Jayakumar, G.L. Clayman, W.L. Di, and K. Mills. 2010. New role for LEKTI in skin barrier formation: label-free quantitative proteomic identification of caspase 14 as a novel target for the protease inhibitor LEKTI. *J. Proteome Res.* 9:4289–4294. http://dx.doi.org/10.1021/pr1003467

Bitoun, E., A. Micheloni, L. Lamant, C. Bonnart, A. Tartaglia-Polcini, C. Cobbold, T. Al Saati, F. Mariotti, J. Mazereeuw-Hautier, F. Boralevi, et al. 2003. LEKTI proteolytic processing in human primary keratinocytes, tissue distribution and defective expression in Netherton syndrome. *Hum. Mol. Genet.* 12:2417–2430. http://dx.doi.org/10.1093/hmg/ddg247

Boniface, K., F.X. Bernard, M. Garcia, A.L. Gurney, J.C. Lecron, and F. Morel. 2005. IL-22 inhibits epidermal differentiation and induces proinflammatory gene expression and migration of human keratinocytes. *J. Immunol.* 174:3695–3702.

Bonnart, C., C. Deraison, M. Lacroix, Y. Uchida, C. Besson, A. Robin, A. Briot, M. Gonthier, L. Lamant, P. Dubus, et al. 2010. Elastase 2 is expressed in human and mouse epidermis and impairs skin barrier function in Netherton syndrome through filaggrin and lipid misprocessing. *J. Clin. Invest.* 120:871–882. http://dx.doi.org/10.1172/JCI41440

Brattsand, M., and T. Egelrud. 1999. Purification, molecular cloning, and expression of a human stratum corneum trypsin-like serine protease with possible function in desquamation. *J. Biol. Chem.* 274:30033–30040. http://dx.doi.org/10.1074/jbc.274.42.30033

Brattsand, M., K. Stefansson, C. Lundh, Y. Haasum, and T. Egelrud. 2005. A proteolytic cascade of kallikreins in the stratum corneum. *J. Invest.*

*Dermatol.* 124:198–203. http://dx.doi.org/10.1111/j.0022-202X.2004.23547.x

Briot, A., C. Deraison, M. Lacroix, C. Bonnart, A. Robin, C. Besson, P. Dubus, and A. Hovnanian. 2009. Kallikrein 5 induces atopic dermatitis-like lesions through PAR2-mediated thymic stromal lymphopoietin expression in Netherton syndrome. *J. Exp. Med.* 206:1135–1147. http://dx.doi.org/10.1084/jem.20082242

Carroll, J.M., and L.B. Taichman. 1992. Characterization of the human involucrin promoter using a transient beta-galactosidase assay. *J. Cell Sci.* 103:925–930.

Carroll, J.M., K.M. Albers, J.A. Garlick, R. Harrington, and L.B. Taichman. 1993. Tissue- and stratum-specific expression of the human involucrin promoter in transgenic mice. *Proc. Natl. Acad. Sci. USA.* 90:10270–10274. http://dx.doi.org/10.1073/pnas.90.21.10270

Caubet, C., N. Jonca, M. Brattsand, M. Guerrin, D. Bernard, R. Schmidt, T. Egelrud, M. Simon, and G. Serre. 2004. Degradation of corneodesmosome proteins by two serine proteases of the kallikrein family, SCTE/KLK5/hK5 and SCCE/KLK7/hK7. *J. Invest. Dermatol.* 122:1235–1244. http://dx.doi.org/10.1111/j.0022-202X.2004.22512.x

Chavanas, S., C. Bodemer, A. Rochat, D. Hamel-Teillac, M. Ali, A.D. Irvine, J.L. Bonafé, J. Wilkinson, A. Taïeb, Y. Barrandon, et al. 2000. Mutations in SPINK5, encoding a serine protease inhibitor, cause Netherton syndrome. *Nat. Genet.* 25:141–142. http://dx.doi.org/10.1038/75977

Comel, M. 1949. Ichthyosis Linearis circumflexa. *Dermatologica.* 98:133–136. http://dx.doi.org/10.1159/000257290

de Veer, S.J., J.E. Swedberg, E.A. Parker, and J.M. Harris. 2012. Non-combinatorial library screening reveals subsite cooperativity and identifies new high-efficiency substrates for kallikrein-related peptidase 14. *Biol. Chem.* 393:331–341. http://dx.doi.org/10.1515/bc-2011-250

de Veer, S.J., S.S. Ukolova, C.A. Munro, J.E. Swedberg, A.M. Buckle, and J.M. Harris. 2013. Mechanism-based selection of a potent kallikrein-related peptidase 7 inhibitor from a versatile library based on the sunflower trypsin inhibitor SFTI-1. *Biopolymers.* 100:510–518.

Denecker, G., E. Hoste, B. Gilbert, T. Hochepied, P. Ovaere, S. Lippens, C. Van den Broecke, P. Van Damme, K. D'Herde, J.P. Hachem, et al. 2007. Caspase-14 protects against epidermal UVB photodamage and water loss. *Nat. Cell Biol.* 9:666–674. http://dx.doi.org/10.1038/ncb1597

Deraison, C., C. Bonnart, F. Lopez, C. Besson, R. Robinson, A. Jayakumar, F. Wagberg, M. Brattsand, J.P. Hachem, G. Leonardsson, and A. Hovnanian. 2007. LEKTI fragments specifically inhibit KLK5, KLK7, and KLK14 and control desquamation through a pH-dependent interaction. *Mol. Biol. Cell.* 18:3607–3619. http://dx.doi.org/10.1091/mbc.E07-02-0124

Descargues, P., C. Deraison, C. Bonnart, M. Kreft, M. Kishibe, A. Ishida-Yamamoto, P. Elias, Y. Barrandon, G. Zambruno, A. Sonnenberg, and A. Hovnanian. 2005. Spink5-deficient mice mimic Netherton syndrome through degradation of desmoglein 1 by epidermal protease hyperactivity. *Nat. Genet.* 37:56–65.

Descargues, P., C. Deraison, C. Prost, S. Fraitag, J. Mazereeuw-Hautier, M. D'Alessio, A. Ishida-Yamamoto, C. Bodemer, G. Zambruno, and A. Hovnanian. 2006. Corneodesmosomal cadherins are preferential targets of stratum corneum trypsin- and chymotrypsin-like hyperactivity in Nethertonsyndrome. *J. Invest. Dermatol.* 126:1622–1632. http://dx.doi.org/10.1038/sj.jid.5700284

Ekholm, I.E., M. Brattsand, and T. Egelrud. 2000. Stratum corneum tryptic enzyme in normal epidermis: a missing link in the desquamation process? *J. Invest. Dermatol.* 114:56–63. http://dx.doi.org/10.1046/j.1523-1747.2000.00820.x

Fortugno, P., A. Bresciani, C. Paolini, C. Pazzagli, M. El Hachem, M. D'Alessio, and G. Zambruno. 2011. Proteolytic activation cascade of the Netherton syndrome-defective protein, LEKTI, in the epidermis: implications for skin homeostasis. *J. Invest. Dermatol.* 131:2223–2232. http://dx.doi.org/10.1038/jid.2011.174

Frateschi, S., E. Camerer, G. Crisante, S. Rieser, M. Membrez, R.P. Charles, F. Beermann, J.C. Stehle, B. Breiden, K. Sandhoff, et al. 2011. PAR2 absence completely rescues inflammation and ichthyosis caused by altered CAP1/Prss8 expression in mouse skin. *Nat Commun.* 2:161. http://dx.doi.org/10.1038/ncomms1162

Guttman-Yassky, E., N. Dhingra, and D.Y. Leung. 2013. New era of biologic therapeutics in atopic dermatitis. *Expert Opin. Biol. Ther.* 13:549–561. http://dx.doi.org/10.1517/14712598.2013.758708

Hansson, L., A. Bäckman, A. Ny, M. Edlund, E. Ekholm, B. Ekstrand Hammarström, J. Törnell, P. Wallbrandt, H. Wennbo, and T. Egelrud. 2002. Epidermal overexpression of stratum corneum chymotryptic enzyme in mice: a model for chronic itchy dermatitis. *J. Invest. Dermatol.* 118:444–449. http://dx.doi.org/10.1046/j.0022-202x.2001.01684.x

Hausser, I., and I. Anton-Lamprecht. 1996. Severe congenital generalized exfoliative erythroderma in newborns and infants: a possible sign of Netherton syndrome. *Pediatr. Dermatol.* 13:183–199. http://dx.doi.org/10.1111/j.1525-1470.1996.tb01202.x

Hewett, D.R., A.L. Simons, N.E. Mangan, H.E. Jolin, S.M. Green, P.G. Fallon, and A.N. McKenzie. 2005. Lethal, neonatal ichthyosis with increased proteolytic processing of filaggrin in a mouse model of Netherton syndrome. *Hum. Mol. Genet.* 14:335–346. http://dx.doi.org/10.1093/hmg/ddi030

Homey, B., and A. Zlotnik. 1999. Chemokines in allergy. *Curr. Opin. Immunol.* 11:626–634. http://dx.doi.org/10.1016/S0952-7915(99)00028-X

Horikawa, T., T. Nakayama, I. Hikita, H. Yamada, R. Fujisawa, T. Bito, S. Harada, A. Fukunaga, D. Chantry, P.W. Gray, et al. 2002. IFN-γ-inducible expression of thymus and activation-regulated chemokine/CCL17 and macrophage-derived chemokine/CCL22 in epidermal keratinocytes and their roles in atopic dermatitis. *Int. Immunol.* 14:767–773. http://dx.doi.org/10.1093/intimm/dxf044

Hoste, E., P. Kemperman, M. Devos, G. Denecker, S. Kezic, N. Yau, B. Gilbert, S. Lippens, P. De Groote, R. Roelandt, et al. 2011. Caspase-14 is required for filaggrin degradation to natural moisturizing factors in the skin. *J. Invest. Dermatol.* 131:2233–2241. http://dx.doi.org/10.1038/jid.2011.153

Hovnanian, A. 2013. Netherton syndrome: skin inflammation and allergy by loss of protease inhibition. *Cell Tissue Res.* 351:289–300. http://dx.doi.org/10.1007/s00441-013-1558-1

Judge, M.R., G. Morgan, and J.I. Harper. 1994. A clinical and immunological study of Netherton's syndrome. *Br. J. Dermatol.* 131:615–621. http://dx.doi.org/10.1111/j.1365-2133.1994.tb04971.x

Kennedy-Crispin, M., E. Billick, H. Mitsui, N. Gulati, H. Fujita, P. Gilleaudeau, M. Sullivan-Whalen, L.M. Johnson-Huang, M. Suárez-Fariñas, and J.G. Krueger. 2012. Human keratinocytes' response to injury upregulates CCL20 and other genes linking innate and adaptive immunity. *J. Invest. Dermatol.* 132:105–113. http://dx.doi.org/10.1038/jid.2011.262

Komatsu, N., K. Saijoh, N. Otsuki, T. Kishi, I.P. Micheal, C.V. Obiezu, C.A. Borgono, K. Takehara, A. Jayakumar, H.K. Wu, et al. 2007. Proteolytic processing of human growth hormone by multiple tissue kallikreins and regulation by the serine protease inhibitor Kazal-Type5 (SPINK5) protein. *Clin. Chim. Acta.* 377:228–236. http://dx.doi.org/10.1016/j.cca.2006.10.009

Lee, E.B., K.W. Kim, J.Y. Hong, H.M. Jee, M.H. Sohn, and K.E. Kim. 2010. Increased serum thymic stromal lymphopoietin in children with atopic dermatitis. *Pediatr. Allergy Immunol.* 21:e457–e460. http://dx.doi.org/10.1111/j.1399-3038.2009.00919.x

List, K., C.C. Haudenschild, R. Szabo, W. Chen, S.M. Wahl, W. Swaim, L.H. Engelholm, N. Behrendt, and T.H. Bugge. 2002. Matriptase/MT-SP1 is required for postnatal survival, epidermal barrier function, hair follicle development, and thymic homeostasis. *Oncogene.* 21:3765–3779. http://dx.doi.org/10.1038/sj.onc.1205502

Mills, K.H., L.S. Dungan, S.A. Jones, and J. Harris. 2013. The role of inflammasome-derived IL-1 in driving IL-17 responses. *J. Leukoc. Biol.* 93:489–497. http://dx.doi.org/10.1189/jlb.1012543

Netherton, E.W. 1958. A unique case of trichorrhexis nodosa; bamboo hairs. *AMA Arch. Derm.* 78:483–487. http://dx.doi.org/10.1001/archderm.1958.01560100059009

Nograles, K.E., L.C. Zaba, E. Guttman-Yassky, J. Fuentes-Duculan, M. Suárez-Fariñas, I. Cardinale, A. Khatcherian, J. Gonzalez, K.C. Pierson, T.R. White, et al. 2008. Th17 cytokines interleukin (IL)-17 and IL-22 modulate distinct inflammatory and keratinocyte-response pathways. *Br. J. Dermatol.* 159:1092–1102.

Oji, V., G. Beljan, K. Beier, H. Traupe, and T.A. Luger. 2005. Topical pimecrolimus: a novel therapeutic option for Netherton syndrome. *Br. J. Dermatol.* 153:1067–1068. http://dx.doi.org/10.1111/j.1365-2133.2005.06884.x

Perera, G.K., P. Di Meglio, and F.O. Nestle. 2012. Psoriasis. *Annu. Rev. Pathol.* 7:385–422. http://dx.doi.org/10.1146/annurev-pathol-011811-132448

Renner, E.D., D. Hartl, S. Rylaarsdam, M.L. Young, L. Monaco-Shawver, G. Kleiner, M.L. Markert, E.R. Stiehm, B.H. Belohradsky, M.P. Upton, et al. 2009. Comèl-Netherton syndrome defined as primary immunodeficiency. *J. Allergy Clin. Immunol.* 124:536–543. http://dx.doi.org/10.1016/j.jaci.2009.06.009

Roth, W., J. Deussing, V.A. Botchkarev, M. Pauly-Evers, P. Saftig, A. Hafner, P. Schmidt, W. Schmahl, J. Scherer, I. Anton-Lamprecht, et al. 2000. Cathepsin L deficiency as molecular defect of furless: hyperproliferation of keratinocytes and pertubation of hair follicle cycling. *FASEB J.* 14:2075–2086. http://dx.doi.org/10.1096/fj.99-0970com

Sakabe, J., M. Yamamoto, S. Hirakawa, A. Motoyama, I. Ohta, K. Tatsuno, T. Ito, K. Kabashima, T. Hibino, and Y. Tokura. 2013. Kallikrein-related peptidase 5 functions in proteolytic processing of profilaggrin in cultured human keratinocytes. *J. Biol. Chem.* 288:17179–17189. http://dx.doi.org/10.1074/jbc.M113.476820

Sales, K.U., A. Masedunskas, A.L. Bey, A.L. Rasmussen, R. Weigert, K. List, R. Szabo, P.A. Overbeek, and T.H. Bugge. 2010. Matriptase initiates activation of epidermal pro-kallikrein and disease onset in a mouse model of Netherton syndrome. *Nat. Genet.* 42:676–683. http://dx.doi.org/10.1038/ng.629

Soumelis, V., P.A. Reche, H. Kanzler, W. Yuan, G. Edward, B. Homey, M. Gilliet, S. Ho, S. Antonenko, A. Lauerma, et al. 2002. Human epithelial cells trigger dendritic cell mediated allergic inflammation by producing TSLP. *Nat. Immunol.* 3:673–680. http://dx.doi.org/10.1038/nrm910

Stefansson, K., M. Brattsand, A. Ny, B. Glas, and T. Egelrud. 2006. Kallikrein-related peptidase 14 may be a major contributor to trypsin-like proteolytic activity in human stratum corneum. *Biol. Chem.* 387:761–768. http://dx.doi.org/10.1515/BC.2006.095

Stefansson, K., M. Brattsand, D. Roosterman, C. Kempkes, G. Bocheva, M. Steinhoff, and T. Egelrud. 2008. Activation of proteinase-activated receptor-2 by human kallikrein-related peptidases. *J. Invest. Dermatol.* 128:18–25. http://dx.doi.org/10.1038/sj.jid.5700965

Steinhoff, M., U. Neisius, A. Ikoma, M. Fartasch, G. Heyer, P.S. Skov, T.A. Luger, and M. Schmelz. 2003. Proteinase-activated receptor-2 mediates itch: a novel pathway for pruritus in human skin. *J. Neurosci.* 23:6176–6180.

Stryk, S., E.C. Siegfried, and A.P. Knutsen. 1999. Selective antibody deficiency to bacterial polysaccharide antigens in patients with Netherton syndrome. *Pediatr. Dermatol.* 16:19–22. http://dx.doi.org/10.1046/j.1525-1470.1999.99005.x

Suárez-Fariñas, M., N. Dhingra, J. Gittler, A. Shemer, I. Cardinale, C. de Guzman Strong, J.G. Krueger, and E. Guttman-Yassky. 2013. Intrinsic atopic dermatitis shows similar TH2 and higher TH17 immune activation compared with extrinsic atopic dermatitis. *J. Allergy Clin. Immunol.* 132:361–370. http://dx.doi.org/10.1016/j.jaci.2013.04.046

Sun, J.D., and K.G. Linden. 2006. Netherton syndrome: a case report and review of the literature. *Int. J. Dermatol.* 45:693–697. http://dx.doi.org/10.1111/j.1365-4632.2005.02637.x

Suzuki, Y., J. Nomura, J. Hori, J. Koyama, M. Takahashi, and I. Horii. 1993. Detection and characterization of endogenous protease associated with desquamation of stratum corneum. *Arch. Dermatol. Res.* 285:372–377. http://dx.doi.org/10.1007/BF00371839

Tsuda, T., M. Tohyama, K. Yamasaki, Y. Shirakata, Y. Yahata, S. Tokumaru, K. Sayama, and K. Hashimoto. 2003. Lack of evidence for TARC/CCL17 production by normal human keratinocytes in vitro. *J. Dermatol. Sci.* 31:37–42. http://dx.doi.org/10.1016/S0923-1811(02)00138-X

Yamasaki, K., J. Schauber, A. Coda, H. Lin, R.A. Dorschner, N.M. Schechter, C. Bonnart, P. Descargues, A. Hovnanian, and R.L. Gallo. 2006. Kallikrein-mediated proteolysis regulates the antimicrobial effects of cathelicidins in skin. *FASEB J.* 20:2068–2080. http://dx.doi.org/10.1096/fj.06-6075com

Yang, T., D. Liang, P.J. Koch, D. Hohl, F. Kheradmand, and P.A. Overbeek. 2004. Epidermal detachment, desmosomal dissociation, and destabilization of corneodesmosin in Spink5$^{-/-}$ mice. *Genes Dev.* 18:2354–2358. http://dx.doi.org/10.1101/gad.1232104